Journal of Ceramic Processing Research. Vol. 23, No. 2, pp. 113~120 (2022)
(Received 27 February 2021, Received in revised form 6 April 2021, Accepted 19 April 2021)
https://doi.org/10.36410/jcpr.2022.23.2.113

J O U R N A L O F
Ceramic Processing Research

Composition and ceramic properties of Meskine (Far-North, Cameroon) ball clays: Potential use as raw materials for tiles making

Soureiyatou Fadil-Djenabou[a,*], Fuh Calistus Gentry[b] and Paul-Desire Ndjigui[b]
[a]*Department of Life and Earth Sciences, Higher Teachers' Training College, University of Maroua, P.O. Box 55 Maroua, Cameroon*
[b]*Department of Earth Sciences, University of Yaoundé I, P.O. Box 812, Yaoundé, Cameroon*

Six samples from Meskine ball clay deposit were investigated to infer their properties, and potential use in the ceramic industry. Characterization of crude clays involved particle size distribution, plasticity, chemical and mineralogical composition. Fired properties of clays were measured in terms of linear shrinkage, bending and compressive strength, bulk density and water absorption. Samples found to be mainly very heavy plastic clays. It appears that the Meskine ball clays are suitable for making solid bricks. The alkali and alkaline earth oxide compositions are moderate with average 7.73 wt.%. Kaolinite is the dominant mineral associated with quartz, smectite, feldspars, goethite, anatase and gibbsite. These mineralogical, physical, chemical and technological features show that Meskine clays are commercial ball clay used in the ceramic industry. At 1100 °C, the fired products are yellowish red. The sound is metallic; bulk density varies between 1.7 and 1.8 Kg/cm^3. Water absorption is below 22%. Bending and compressive strength are slightly higher with respective average of 22.66 Mpa and 40.06 Mpa. All these parameters compared to the Italian standards reveal that the Meskine clays are suitable for the manufacture of wall tiles, floor tiles and for roof tiles.

Key words: ball clays, Composition, Ceramic tiles, Meskine, Far-North Cameroon.

Introduction

Ball clays are plastic clays and mainly composed of kaolinite (25-80%), illite and micas (10-30%), mixed with smectite and small amount of organic matter [1, 2]. These features influence the physical and mechanical properties of raw materials [3-5]. Around 14% of ball clays used in floor and wall tiles production to give better particle size distribution for better density and whiteness to the product. Ball clays are also essential in-tile bodies for plasticity and work-ability for pressing and unfired strength required for handling of pressed tiles. A high content of fine grain size particle is inversely proportional to surface area and plasticity of ball clays. They should demonstrate high bending strength after drying at 110 °C, sometimes between 8 and 10 Mpa, and high specific areas of 20-50 m^2/g. Due to these features optimal plastic ball clays ought to have good sintering properties, as the phase transitions of clay minerals start at relatively low temperatures. Such clay materials are highly reactive towards other components of the ceramic. They process perfect physical and mechanical properties batch for tile production, especially against feldspars [2, 6-8]. The flexural strength values are more than 6.5 MPa for tiles [9]. The ceramic tile industry was quickly developing in recent years, especially in African countries like Benin, Ivory Coast, Senegal, Togo, South Africa, Cameroon, and Namibia. This will help lift the economies of these countries. Meskine ball clays have been used more than 30 years in the production of common bricks and pottery. Unfortunately lack of knowledge of their composition slows down their industrialization. To permit their valorization knowledge of their composition and ceramic properties is necessary.

*Corresponding author:
Tel : +237694420883
Fax: +22291988
E-mail: soureiyatou@yahoo.fr

Geographical and Geological Setting

Meskine region is situated between 10°32' and 10°33'N, and 14°13' and 14°14'E, North of Maroua Subdivision and Diamaré Division, in the Far North Region (Fig. 1). This region is characterized by a dry tropical climate of the Sudano Sahelian type, characterized by two seasons: a rainy season that last four months, from June to September; and a long dry season, which extends from October to May. These seasons are marked by winds such as the Monsoon of west-east direction (it blows from May to September) and the Harmattan, hot and dry wind (it blows from the north towards the south from October until April). The relief of Meskine is characterized by a set of plains and mountains, and it is little rugged. We mainly find external karals (320-360 m) and ancient alluvium.

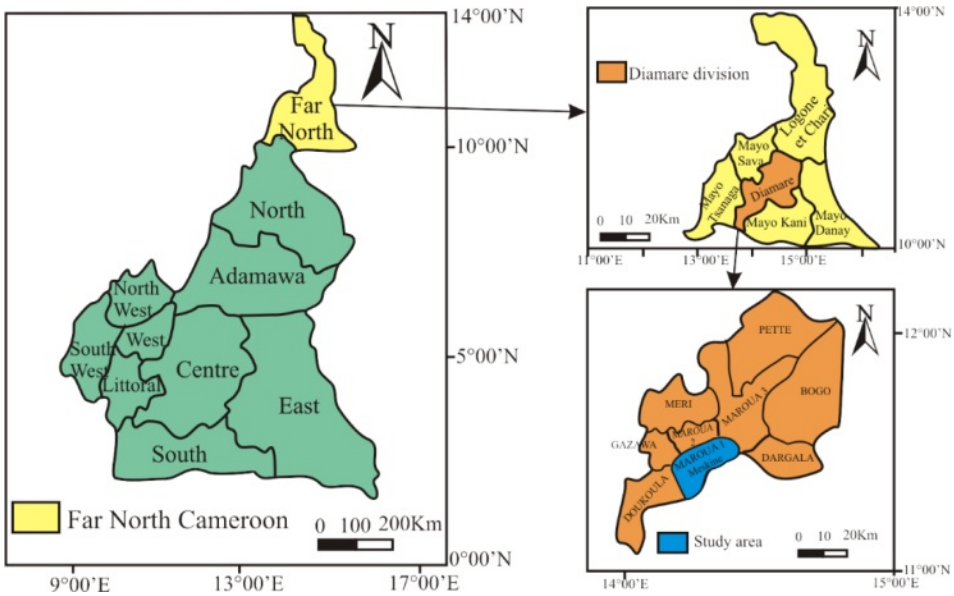

Fig. 1. Location map of the study area (OpenstreetMap and field data).

Indeed, Meskine consist of plain surmounted by two mountains: Mount Makabaye and Mount Yamdjidjim [10-13]. The cover vegetation is the shrub savanna. The flora is quite diversified and there are species such as *Acacia seyal*, *Acacia hockii*, *Ziziphus mauritiana*, *Combretum nigricans* and *Balanites aegyptiaca*. There is also the notorious presence of Neem (*Azradirachtaindica*) [14]. A single seasonal watercourse named Mayo Kaliao crosses this region. This watercourse is fed by the passage of water from the surrounding mountains. During the dry season, in the bed of these watercourses, there is a subsurface flow, allowing the water supply of local populations. There are little evolved soils on recent alluvia, coarse sands, and little moist soil [15]. We note: bare soils, with clay texture found in karals; soils with sand-clay texture; and alluvial soils with sandy-silty texture, which are found in the plains and especially on the edges of the mayos (seasonal rivers), and which constitute the support of an intense agricultural activity. These soils are very suitable for growing onions, traditional vegetables and tomatoes. The Extreme-North region of Cameroon consists of a Precambrian basement on which unconformity with sub horizontal sedimentary rocks of Mesozoic and Cenozoic age. An epimetamorphic set covering about 5% of the basement surface forms a band north of Maroua [11]. This region is made up of several geological formations of various origins: volcanic, plutonic, metamorphic and sedimentary. In addition to these four formations, we also find recent alluvia. They are sands, clayey and silty sands, decantation clays which are products of weathered debris carried off by runoff from the Mandara Mountains and forming alluvial placers in the Mayo Tsanaga and Kaliao and the Logone River [16]. Alluviums cover a large part of the region as well as the study area.

Materials and Methods

Samples and sampling techniques

Six bulk samples were collected from two vertical sections subdivided into three layers in in the Meskine alluvial terrace. The clay material is traditionally used in pottery and common bricks by local population. Samples were designated for the first section MK1a for the base, MK1b for the middle layer and MK1c for the top layer. The second profile is located on the diagonal of the first one. Samples were designed MK2a for the base, MK2b for the middle layer and MK2c for the top layer.

Analytical techniques

Particle size distribution (PSD) was obtained by sieving for the coarse and fine sandy fractions using sieves of 200 and 50 µm respectively. The silty and clayey fractions were obtained using Robinson's pipette method. Colors of raw materials were determined using the Munsell Soil Color Book [17]. Atterberg's Consistency liquid limit (Ll) and plastic limit (Pl) was carried out using the Casagrande apparatus [18].

The mineralogical assemblage was determined by X-ray Diffraction (XRD) analysis using a D8 advanced Bruker diffractometer equipped with a Co Kα radiation (λ = 1.7890 Å) operating at 35 kV and 45 mA. The diffraction patterns were obtained from 1.5° to 32° at a scanning rate of $1°min^{-1}$. Infra-red spectra were recorded in diffuse reflectance mode using a Bruker Fourier Transform Interferometer IFS 55. The spectra, recorded from 4000 cm^{-1} to 600 cm^{-1} with a resolution of 4 cm^{-1}, are obtained by accumulation of 200 scans.

The concentrations of major elements were determined using X-ray fluorescence after being heated and melted with a flux of lithium tetraborate and analyzed using a

Pan Analytical Axios Advanced PW4400.

Technological properties were determined on test briquettes (with dimensions 80×40×10.4 mm) obtained by compressing humidified crushed clayey material with a SPECAC laboratory hydraulic press of 10 ton. The added water, for humidification, was in a weight percentage of 7-15%, with respect to the clayey material. The briquette specimens were placed on a wooden board for 24 hours for natural drying, followed by oven drying at 105 ºC for 24 hours to eliminate absorbed water. After oven drying, the specimens were fired in a Nobertherm programmable electric furnace at 900, 1000 and 1100 ºC. The firing profile was as follows, 4 ºC/min from 23 ºC up to 580 ºC, and 5 ºC/min from 580 ºC up to the final temperatures. Each sample is left to equilibrate for 2 hours at 580º, before the following heating sequence. After soaking for 30 min at each final temperature, the specimens were furnace-cooled to room temperature at 900, 1000 and 1100 ºC. Color of fired briquettes was appreciated in the same way as raw samples. Cohesion was tested manually by breaking the briquettes. Sound test was done by knocking the fired specimens with a metal rod. The densification parameters of the fired briquettes were accessed by measuring linear shrinkage; weight loss; water absorption capacity and bulk density [19]. Ceramic tiles were prepared using clay materials that were semi-pressed (humidity:7 wt% of water, shaping pressure 15-25 Mpa, dimension 50×100 mm) and then fired in electric furnace, 1h dwell time and 5 ºC/min heating rate). The linear shrinkage, water absorption and bending strength of fired samples were measured following standard the ASTM procedures (20). Test specimens were prepared by the pressing technique at a pressure of 19.6 MPa using (15×15×7) cm molds and then dried at 110 ºC for 24 h. The specimens were fired in an Electric Lavoisier 460 D furnace with a 7 ºC/min heating rate at temperature of 1100 ºC for 60 min, followed by natural cooling to room temperature. To simulate the conditions of formation of color inhomogeneities, the tile specimens have been chemically treated by immersion in 100 mL muriatic acid without dilution for 8 days at room temperature. After that the densification behavior was studied by same method for raw materials.

Results and Discussion

Raw material characterization

Particle size distribution and Atterberg's limits

Table 1 shows grain size particles of samples; there is variable proportion of particles. Clay particle proportion varies between 23.54 and 58.29%, with lower value in MK1c sample and higher one in MK2c sample. Silt particles are higher in all samples with average of 36.29%. At the same times, sand particles are very low, with average of 5.04%. The studied materials are characterized by very heavy clayey texture except MK1c sample (Fig. 2). The Meskine ball clays are suitable for making solid bricks except the heavy silty sample (Fig. 3). The plasticity diagram shows that the MK1b and MK2b samples are moderately clayey and very plastic, MK2a and MK2c are clayey and very plastic, MK1c is very plastic and MK1a is low plastic (Fig. 4).

Mineralogical and chemical composition

Meskine ball clay samples mainly consist of illite (30-50%), kaolinite (10-32%), smectite (2-14%), quartz (3-17%), and few amounts of feldspars, goethite, anatase and gibbsite (Table 2). The infra-red absorption spectra

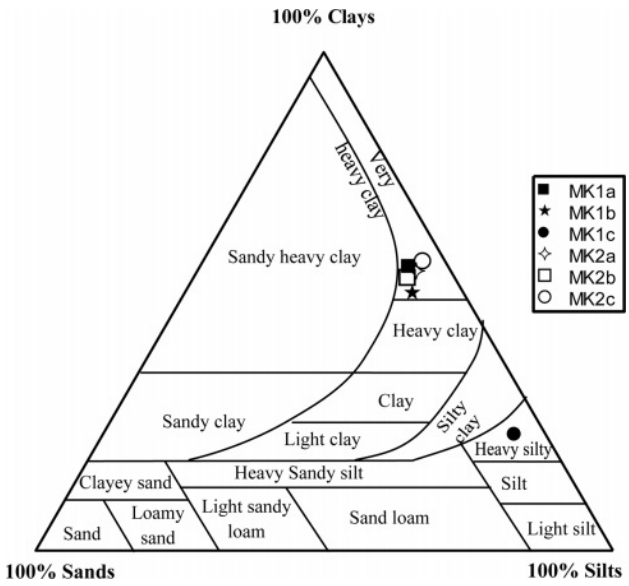

Fig. 2. Ternary diagram

Table 1. Color variation, particle grains distribution and Atterberg's limits of Meskine ball clay

Samples	MK1a	MK1b	MK1c	MK2a	MK2b	MK2c
Munsell code	10YR3/2	10YR4/6	10YR2/2	10YR3/1	10YR3/2	10YR2/2
Color	Grayish brown	Reddish brown	Dark gray	Gray	Grayish brown	Dark gray
Sands (%)	6,94	9,01	5,59	6,07	8,52	4,05
Silts (%)	35,84	39,02	70,87	37,61	36,63	37,65
Clays (%)	57,22	51,95	23,54	56,32	54,85	58,29
Ll	31,8	51,3	68,5	55,0	52,4	57,0
Pl	23,4	24,6	27,1	28,1	25,2	24,6
Pi	8,4	26,7	41,4	26,9	27,2	32,4

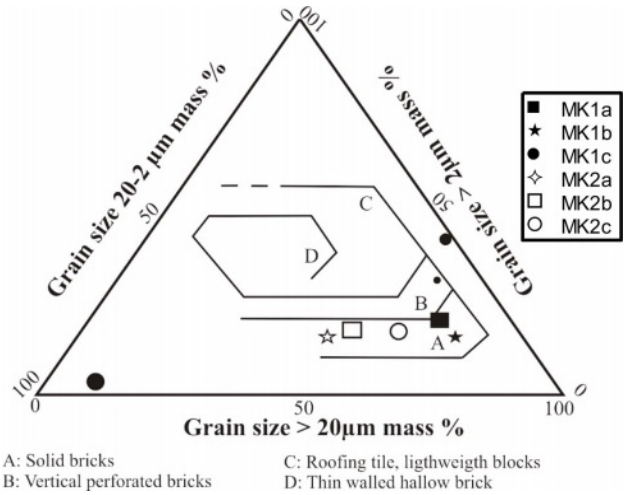

Fig. 3. Winkler diagram (Winkler, 1954).

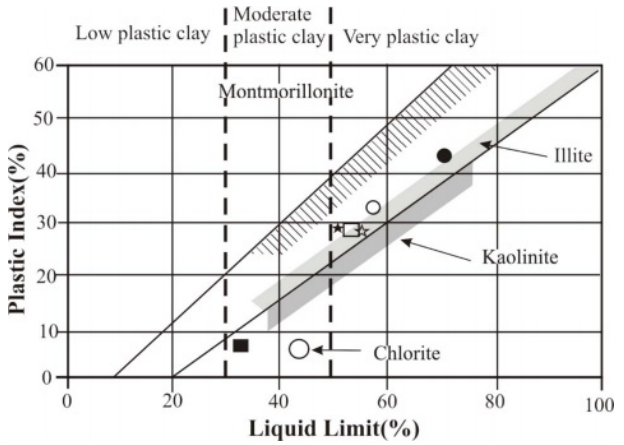

Fig. 4. Position of Meskine ball clay in the Holtz and Kovacs plasticity chart

Table 2. Bulk mineralogy (%) of Meskine ball clays

Samples	MK1a	MK1b	MK1c	MK2a	MK2b	MK2c
illite	50	33	34	30	31	36
smectites	2	3	14	5	13	13
kaolinite	13	30	18	32	28	15
quartz	17	15	8	14	3	4
anatase	8	8	14	10	15	17
feldspars	1	2	3	3	2	3
goethite	0	2	3	0	1	5
gibbsite	3	2	2	1	0	2

(Fig. 5) show a sharp band around 3635 cm^{-1} due to OH stretching bands, usually observed in kaolinite [23, 24]. A broad band of water is observed around 3416 cm^{-1} due to overlapping asymmetric υ_3 and symmetric υ_1 (H-O-H) stretching of H- bonded water [25, 26]. The stretching and bending of hydration water are observed at 1637-1633 cm^{-1} [25]. The Si-O stretching band of smectite is observed at 1875-1045 cm^{-1}. The bands near 1985 cm^{-1} are combinations of SiO_2 impurities. The

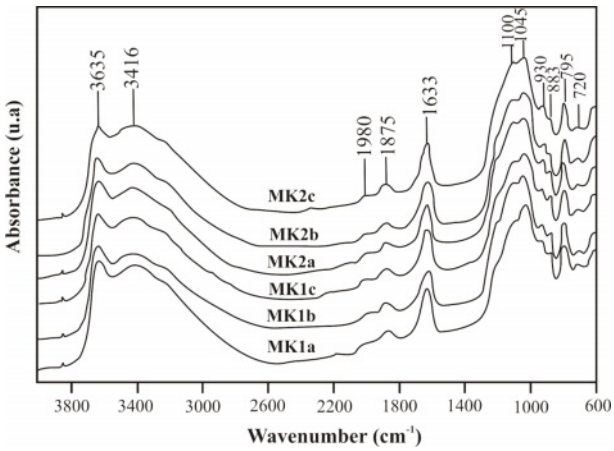

Fig. 5. Infra-Red spectrum of samples.

bands of 720, 795 and 1980 cm^{-1} may be all ascribed to cristobalite [27]. The band observed at 883 cm^{-1} is assigned to the deformation δOH of AlFe-OH. The presence of goethite could also indicate a detrital origin [5, 28]. Illite is formed by hydrolysis of feldspars [29]. Absorption bands of low intensity centered around 1632 cm^{-1} on all studied materials might be attributed to water molecules or optionally to other radical constituents of amorphous alumino-silicates. The mineral assemblage of the raw materials can be linked to chemical weathering system of the parent rock, characteristic of Sudano Sahelian region. Smectite associated with kaolinite are found in alluvial deposits under a tropical climate with a contrasting dry season, this would also be related to drainage but also to the rate of soil erodibility [5, 30]. The formation of kaolinite may be due to the supergene precipitation of silica and alumina or the weathering of silicate minerals [31, 32].

The chemical composition of the Meskine ball clays (Table 3) indicates moderate contents in SiO_2 (56-65 wt.%) which are in accordance with the proportion of relic primary silicate as well as secondary siliciclastic minerals [33]. Al_2O_3 contents are rather moderate (15-18 wt.%) and are supported by clay minerals and relic feldspars. Fe_2O_3 contents (av. = 5.24 wt.%) are high, and the alkali (K_2O + Na_2O) and alkali earth (MgO + CaO) contents are moderate. Other oxides such as MnO, TiO_2 and P_2O_5 are very low and below to the detection limit (Table 3). The Meskine ball clays are suitable for making sandstones and tiles (Fig. 6). While the chemical diagram [33] shows that, there are commercial ball clays, suitable in ceramic industry (Fig. 7). The low ferromagnesian contents confirm the moderate chemical weathering [34]. The Loss on Ignition (LOI) values are all less than 13 wt.% and might be linked to the presence of hydrous clay minerals [35-37]. The presence of MgO could favor the production of vitreous phases [35]. Anatase is confirmed by the presence of titanium oxide in variable proportion [38].

Table 3. Major components of Meskine ball clay samples

Major elements (%)	Samples						
	d.l	MK1a	MK1b	MK1c	MK2a	MK2b	MK2c
SiO_2	0.04	58.48	58.32	54.58	65.15	54.35	52.86
Al_2O_3	0.02	16.95	17.15	18.06	15.47	18.35	18.12
Fe_2O_3	0.01	5.32	5.56	6.39	3.24	6.52	6.43
MnO	0.002	0.075	0.086	0.113	0.058	0.117	0.147
MgO	0.01	1.16	1.24	1.33	0.74	1.40	1.5
CaO	0.006	1.430	1.501	1.480	1.684	1.378	2.242
Na_2O	0.02	1.82	1.81	1.54	2.58	1.65	1.38
K_2O	0.01	3.02	2.97	2.7	3.85	2.77	2.56
TiO_2	0.01	1.01	1.02	1.06	0.76	1.11	1.08
P_2O_5	0.002	0.131	0.123	0.127	0.121	0.117	0.099
LOI	0.05	9.51	9.3	11.35	4.81	10.68	12.31
Sum	–	98.91	99.08	98.73	98.46	98.44	98.73
SiO_2/ Al_2O_3	–	3.45	3.40	3.02	4.21	2.96	2.93

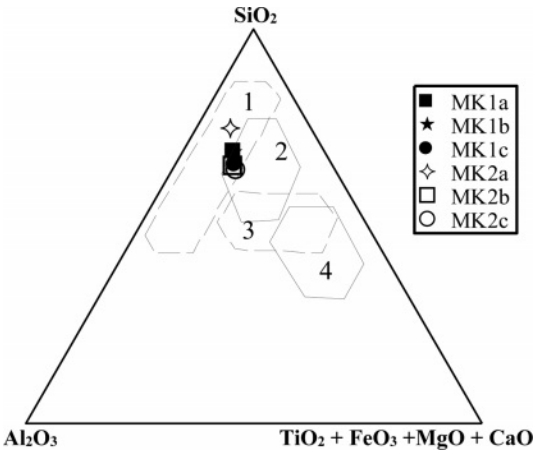

Fig. 6. Diagram of Fiori et al., 1989 showing the chemical composition of domains for tiles, sandstone (1 & 2) and porous tiles (3 & 4)

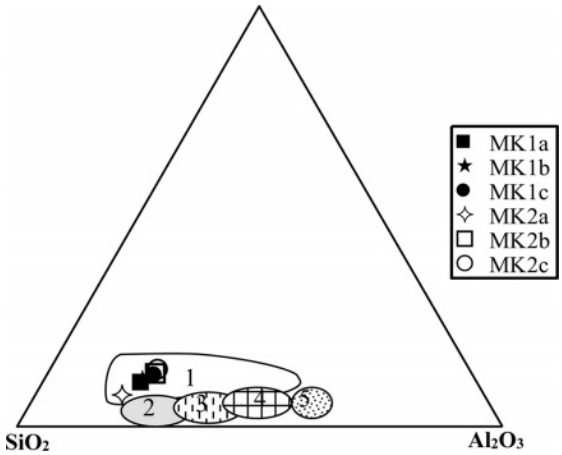

Fig. 7. Chemical Classification Chart of Ligas et al., 1997; 1: commercial ball clays; 2: Kaolin from Italy; 3, 4 Germany; 5: UK

Ceramic test of clay samples

Table 4 shows the values of linear shrinkage, water absorption and color and bulk density of the fired bodies. Linear shrinkage increases with temperature, indeed for 800 ºC to 1100 ºC values of linear shrinkage increases with average of 3.61% for all the samples. At 1100 ºC, significant changes were observed; this is due to the starting of glassy phase formation. The bulk values ranged between 1.57 and 1.78, and at 800 to 900 ºC. These values increase to 1.89 Kg/cm^3 with the firing temperature. The low values of bulk density might be probably due to the low sintering. Water absorption decreases with firing temperature (Table 4). This is linked to glassy phase formation, additionally the presence of oxides could act as fluxing agents enhancing densification [39]. The decrease is more marked at 1100 ºC. The water absorption at 1000 and 1100 ºC is <20% indicating that the Meskine ball clays can be used for brick and roofing tiles. This decrease is due to the sintering of solid-phase materials [40-42]. This could induce a decrease in the porosity, which appeared during the compaction of the clay particles. Generally, water absorption, less than 25%, is good for tiles manufacture [9]. According to the progress of shrinkage with sintering temperature is then stronger for heavy clayed samples (≈5%), above 1100 ºC. As the sintering temperature increases, the density and strength are increasing, while the water absorption and porosity decreases. These analyses closely agrees with the studies of Onwona-Agyeman et al. on clay materials from Ghana [43].

Quality test of tiles

Test specimens were prepared at firing temperatures of 1100 ºC; the results show yellowish red color whatever the sample (Table 4). The red color is probably due to the transformation of goethite into hematite [41]. The yellow color may be linked to the presence of goethite or titane oxide minerals such as anatase in the raw materials [38, 43]. The sound is metallic due to the high proportion of fine particles which induce a good vitrification [43, 44]. The water absorption of all our tiles is greater than 10% this allows us to have wall

Table 4. Technological properties of raw material and tiles prepared from Meskine ball clay

Raw materials							
Samples		MK1a	MK1b	MK1c	MK2a	MK2b	MK2c
800 °C	Color	grayish brown	grayish brown	light brown	grayish brown	grayish brown	light brown
	LS(%)	0.58	0.7	0.42	0.40	0.39	0.50
	WA(%)	17.1	17.5	16.4	15.2	14.6	15.2
	Bd(Kg/cm^3)	1.66	1.63	1.65	1.61	1.58	1.57
900 °C	Color	light brown	light brown	dark brown	light brown	light brown	dark brown
	LS	1.69	1.9	1.3	1.2	1.7	1.3
	WA	13.7	15.4	14.3	14.6	15.3	15.6
	Bd	1.78	1.75	1.76	1.73	1.61	1.57
1000 °C	Color	reddish brown	reddish brown	reddish brown	rbrown	rbrown	reddish brown
	LS	2.3	2.1	2.9	2.0	2.7	2.2
	WA	12.8	8.1	7.8	10.7	13.1	9.3
	Bd	1.66	1.63	1.65	1.61	1.58	1.55
1100 °C	Color	yellowish red	yellowish red	yellowish red	yellowish red	yellowish red	yellowish red
	LS	3.6	4.5	4.2	3.6	4.7	4.2
	WA	10.6	7.6	6.1	9.7	11.7	6.2
	Bd	1.89	1.84	1.87	1.85	1.78	1.76
Properties of tiles							
1100 °C	Color	yellowish red	yellowish red	yellowish red	yellowish red	yellowish red	yellowish red
	Sound	Metalic	Metalic	metalic	metalic	metalic	Metalic
	WA	10.6	7.6	6.1	9.7	4.7	4.2
	BS(Mpa)	15.0	32.00	25.00	17.00	24.00	23.00
	CS(Mpa)	22,8	18.59	56.12	45.00	53.75	43.75

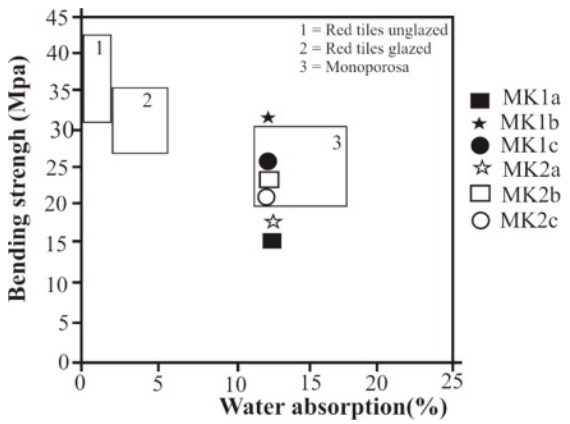

Fig. 8. Relationship between water absorption and bending strength of Meskine tiles and comparison with some commercial products.

tiles, these tiles are also resistant to abrasion according to the standards [45-47]. According to ASTM, 2000. C 20-00 standards, tiles with water absorption values higher than 10% are classified as porous wall tiles [18]. The decreasing of water absorption would be related to the appearance of the glassy phase. The linear shrinkage values for tests tiles are relatively low; they are less than 5% for all samples. These values are favor for ceramic tiles [47, 48]. As the vitrification takes place, the apparent porosity of the product gradually decreases

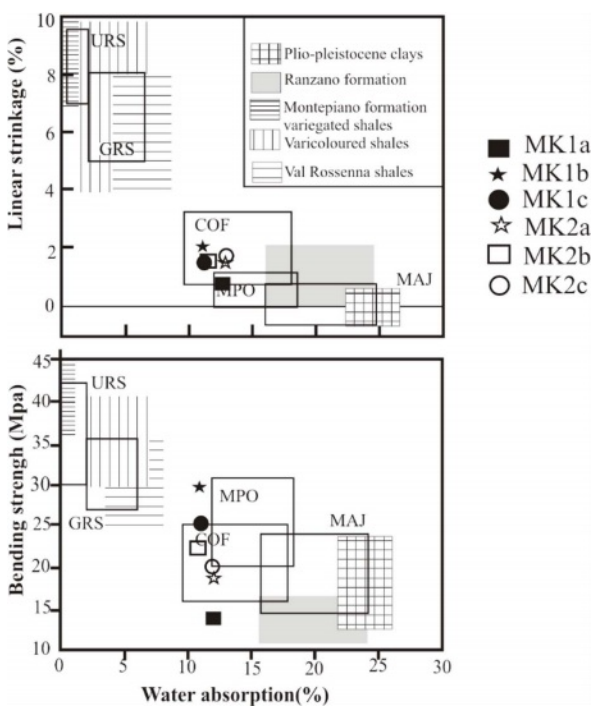

Fig. 9. Technological properties of the products obtained with Meskine ball clay materials in comparison with the requirements of the various types of ceramic tiles. Water absorption versus linear shrinkage A and bending strength B. MAJ: majolica, COF: "cottoforte", MPO: "monoporosa", GRS: glazed red stoneware, URS: unglazed red stoneware.

in order to increase the mechanical strength. Bending and compressive strength are slightly higher for tests tiles (Table 4). These higher values, with average of (22.66 MPa) for bending and (40.06 MPa) for compressive strength, are good for tiles making [46]. This would be because these samples are rich in fine particles. The densification of the tiles due to the presence of flux agents as temperature increased are responsible for the improved compressive strength values recorded [39]. The mechanical properties increase with the baking temperature until the vitreous phase reaches an optimum proportion. This leads us to believe that the bending strength of raw materials can still increase with the firing temperature. The concurrent presence of alkaline and alkaline earth oxides promotes the development of a less viscous liquid phase, which improves the densification kinetics of floor tiles at sufficiently high temperatures [49-51]. In addition, the presence of illite and smectite and the elaborate mixture improve the plasticity are favorable for the appearance of the glassy phases, which increase densification and bending strength [52]. Decomposition of illite and smectite at lower temperatures than in the case of kaolinite also strongly influences sinterability of the formed ceramic material [53]. There was found a good correlation between water absorption after firing at 1000 °C and total illite and smectite content [54, 55]. The inert materials, mainly quartz and feldspars, increase the refractoriness of wall tile bodies, reduce linear shrinkage during firing and regulate the SiO_2/Al_2O_3 ratio, which is an important parameter for densification [56]. Magnesium oxide lowers the maturing temperature, reduces porosity and increases strength [57]. Beyond the critical or optimum value, any increase in temperature will lead to a decrease in bending strength. If the temperature is further increased, the bending strength of specimens could increase [43, 9]. Figures 8 and 9 reveal specific applications for these clays. To make these types of tiles with sample MK1b it is necessary to reduce the bending strength for 8 MPa. For the MK1a sample it is necessary to increase the bending strength of 5 MPa, on the other hand roofing tiles can be obtained with MK1a because its resistance to bending is between 10-20 MPa, water absorption between 10-26%, and linear shrinkage less than 2% [47].

Conclusions

The results obtained from the studied Meskine ball clays show that the ceramic properties obtained on the experimental tiles, depend on the chemical, mineralogical and physical characteristics of our materials. A yellowish red color is observed for all the samples due to the presence of iron oxide and anatase and/or the high content of calcium oxide. Alkali and alkali earth contents are moderate and these could reduce firing temperature. Vitrification is obtained at 1100 °C; with bulk, density varies between 1.7 and 1.8 Kg/cm^3. It is found that, we could have wall tiles, soil tiles and roofing tiles just by adjusting firing temperature.

Acknowledgements

This work was partially supported by the Geoscience Laboratories (Sudbury, Canada). The authors are grateful to team manager of the Cameroon Local Promotion Mission for providing logistic facilities during the fieldwork.

References

1. I.R. Wilson, Ceram. 287[44] (1998) 88-117.
2. M.F. Abadir, and E.H. Sallam, I.M. Bakr. Ceram. Int. 28 (2002) 303-310.
3. S. Ferrari and A.F. Gualtieri, Appl. Clay. Sci. 32 (2006) 73-81.
4. K. Galos. Appl. Clay. Sci. 51[1-2] (2011) 74-85.
5. S. Fadil-Djenabou, in Ph.D Thesis (Fac. Sci. Univ. Press, 2015) p.155.
6. L. Stoch and K. Bahranowski, Geol. Quatr. 20[4] (1976) 807-822.
7. C. Leonelli, F. Bondioli, P. Veronesi, M. Romagnoli, T. Manfredini, G.C. Pellacani, and V. Canillo, J. Euro. Cerm. Sty. 21 (2001) 785-793.
8. M. Dondi, G. Guarini, M. Raimondo, and F. Salucci, Tile Brick. Int. 20[2] (2003) 2-11.
9. B. Tillement, Bull. Dir. Mines et Géol., Camer. Int. 20 (1970) 2-11.
10. J.C. Dumort and Y. Péronné, in "Carte géologique de reconnaissance 1/500 000 - feuille de Maroua Dir Min Géol- Yndé" (Notice explicative, 1966) p.67.
11. M. Detay, in "Atlas de la province de l'Extrême-Nord Cameroun" (IRD. MINREST, 2000) pp.30-37.
12. B.N. Ngatcha, R. Nijtchoua, and E. Naah, in Séminaire International, Bamako (MLI), 2000/06/20-23. ISBN 2-7099-1480-8 ISSN 0767-2896. pp.455-474.
13. R. Letouzey, in "Carte phytogéographique du Cameroun au 1/500000, Domaine sahélien et soudanien" (IRA, Herbier National, 1985) pp.2-9.
14. C. Seignobos, Cahiers Sc 11 (1993) 9-28.
15. P. Ségalen, Cah. ORSTOM, Sér. Pédol (1967) 137-187.
16. Munsell Color, 2000. Charts.Macbeth Div Kollmorge Corp, 2441 North Calvert Strt Baltimore, Maryland 21218, p.29.
17. H. Casagrande, Trans. Am. Soc. Civil Eng. 73 (1947) 783-811.
18. ASTM, No. C20-00 (2000) p.2-3.
19. ASTM, NO. C 674-77 (1997) p.13-14.
20. B. Bah, P. Engels, and G. Collinet, in "Légende de la carte numérique des sols de Wallonie (Belgique)" (Faculté universitaire des Sciences agronomiques de Gembloux , 2005) p.55.
21. H.G.F. Winkler 31 (1954) 337-343.
22. V.S. Olejnik, L.A.G. Aylmore, A.M. Posner, and J.P. Quirk, J. Phys. Chem. 72[1] (1968) 241-249.
23. R.L. Frost, E. Makó, J. Kristóf, E. Horváth, and J.T. Kloprogge, J. Colloid Interface Sci. 239 (2001) 458-466.
24. M. Hajjaji, S. Kacim, and M. Boulmane, Appl Clay Sci. 21 (2001) 203-212.
25. J. Madejová, Vibr. Spec. 31 (2003) 1-10.
26. H. Graetsch, H. Gies, and I. Topalović, Phys. Chem. Miner.

21[3] (1994) 166-175.
27. B.K. Das, A.S. Al-Mikihlafi, and P. Kaur, J. As. Earth. Sci. 26 (2006) 640-668.
28. J. Andigué, L.B. Baohoutou, B. Moupeng, K. Passiring, H. N. Ouaga, and J. Riser, ORSTOM, 12[3] (2001) 149-155.
29. B. Velde, in "Introduction to clay minerals" (Chap Hall, 1992) p.193.
30. P.-D. Ndjigui, P. Bilong, D. Bitom, and A. Dia, J. Afr. Earth Sci. 50 (2008) 305-328.
31. C.M.F. Vieira, R. Sanchez, and S.N. Monteiro, Constr. Build. Mat. 22 (2008) 781-787.
32. P. Ligas, I. Uras, M. Dondi, and M. Marsigli, Appl. Clay. Sci. 12 (1997) 145-163.
33. D.A.C. Manning, in "Introduction to industrial mineral". (Chap & Hall Eds, 1995) p.275.
34. G.E. Christidis, in "Advances in the Characterization of Industrial Minerals" (EMU Notes in Mineralogy, 2011) p.341-414.
35. E. Kamseu, C. Leonelli, D.N. Boccaccini, P. Veronesi, P. Miselli, G. Pellacani, and C. Melo, Ceram. Int. 33 (2007) 851-857.
36. H. Baccour, M. Medhioub, F. Jamoussi, T. Mhiri, and A. Daoud, South, Tu. Materials Charac. 59[11] (2008) 1613-1622.
37. P. Pialy, C. Nkoumbou, F. Villiéras, A. Razafitianamaharav, O. Barres, M. Pelletier, G. Ollivier, I. Bihannic, D. Njopwouo, J. Yvon, and J.-P. Bonnet, Clay Miner 43 (2008) 415-435.
38. A. Andrews, S.K.Y. Gawu, and P.A. Olubambi, J. Ceram. Process. Res. 16 (2015) 37-40.
39. F.A.C. Milheiro, M.N. Freire, A.G.P. Silva, and J.N.F. Holoanda, Ceram. Int. 31 (2006) 757-763.
40. S.J.G Sousa and J.N.F Holanda, Ceram. Int. 31 (2005) 215-222.
41. P. Boch, 2001. Frittage et microstructures des céramiques: Materiaux et processus céramiques. In par Boch P.(Ed), Paris, Hermes, Sciences publications.
42. B. Onwona-Agyeman, A. Yaya, A. Nzihou, N. Lyczko, and D.P. Minh, J. Ceram. Process. Res. 21 (2020) 35-41.
43. S. Fadil-Djenabou and P. -D. Ndjigui, J. A. Mbey 3 (2015) 50-58.
44. C.U. Melo, E. Kamseu, and C. Kamseu, Tiles & Bricks Internat. 19[6] (2003) 57-69.
45. European Standards No. NF EN 14411 (2004) p.76.
46. European Standards No. EN 99:1991 (1994) p.4.
47. ISO, No. 10545-4 (2004) p.6.
48. M. Dondi, M. Marsigli, and I. Venturi, British; Ceram Transac. 98[1] (1999) 12-18.
49. K. Michailidis, G. Trontzios, and E. Sofianska, in Proceedings of the 12th International Congress, May 2010, edited by Bulletin of the Geological Society of Greece (2010) p.8.
50. B.E. Yekta and P. Alizadeh, Am. Ceram. Soc. Bull. 75[5] (1996) 84-86
51. Ö. Cenziz and A. Kara, J. Ceram. Process. Res. 19 (2018) 189-197.
52. M. Hajjaji, S. Kacim, and M. Boulmane, Appl. Clay Sci. 21 (2002) 203-212.
53. W. Hajjaji, M. Hachani, M. Bechir, K. Jeridi, M. Medhioub, A. Lopez-Galindo, F. Rocha, J. A. Labrincha, and F. Jamoussi, J. Afr. Earth Sci. 57 (2010) 41-46.
54. J. Liebermann and W. Schulle, Ceramic Forum International (Ber. DKG) 76[10] (1999) 31-34.
55. A. Aras. Appl. Clay. Sci. 24 (2004) 257-269.
56. E. SANCHEZ, J. GARCIA, Y. SANZ, AND E. OCHANDlO, Tile and Brick Int. 6(4) (1990) 15-21.